

Chapter 6

Future Climate: Projected Average

COORDINATING LEAD AUTHOR

Daniel R. Cayan (Scripps Institution of Oceanography, University of California, San Diego and U.S. Geological Survey)

LEAD AUTHORS

Mary Tyree (Scripps Institution of Oceanography, University of California, San Diego), Kenneth E. Kunkel (NOAA Cooperative Institute for Climate and Satellites, North Carolina State University and National Climate Data Center), Chris Castro (University of Arizona), Alexander Gershunov (Scripps Institution of Oceanography, University of California, San Diego), Joseph Barsugli (University of Colorado, Boulder, CIRES), Andrea J. Ray (NOAA), Jonathan Overpeck (University of Arizona), Michael Anderson (California Department of Water Resources), Joellen Russell (University of Arizona), Balaji Rajagopalan (University of Colorado), Imtiaz Rangwala (University Corporation for Atmospheric Research), Phil Duffy (Lawrence Livermore National Laboratory)

EXPERT REVIEW EDITOR

Mathew Barlow (University of Massachusetts, Lowell)

Executive Summary

This chapter describes possible climate changes projected to evolve during the twenty-first century for the Southwest United States, as compared to recent historical climate. It focuses on how climate change might affect longer-term aspects of the climate in the

Chapter citation: Cayan, D., M. Tyree, K. E. Kunkel, C. Castro, A. Gershunov, J. Barsugli, A. J. Ray, J. Overpeck, M. Anderson, J. Russell, B. Rajagopalan, I. Rangwala, and P. Duffy. 2013. "Future Climate: Projected Average." In *Assessment of Climate Change in the Southwest United States: A Report Prepared for the National Climate Assessment*, edited by G. Garfin, A. Jardine, R. Merideth, M. Black, and S. LeRoy, 101–125. A report by the Southwest Climate Alliance. Washington, DC: Island Press.

Southwest and is closely related to Chapter 7, which is concerned with the implications of climate change on shorter period phenomena, especially extreme events. The projections derive from the outcomes of several global climate models, and associated “downscaled” regional climate simulations, using two emissions scenarios (“A2” or “high-emissions,” and “B1” or “low-emissions”) developed by the Intergovernmental Panel on Climate Change (IPCC) *Special Report on Emissions Scenarios* (SRES; Nakićenović and Swart 2000). The key findings are:

- Temperatures at the earth’s surface in the Southwest will rise substantially (by more than 3°F [1.7°C] over recent historical averages) over the twenty-first century from 2001–2100. (high confidence)
- The amount of temperature rise at the earth’s surface in the Southwest will be higher in summer and fall than winter and spring. (medium-high confidence)
- Climate variations of temperature and precipitation over short periods (year-to-year and decade-to-decade) will continue to be a prominent feature of the Southwest climate. (high confidence)
- There will be lower precipitation in the southern portion of the Southwest region and little change or increasing precipitation in the northern portion. (medium-low confidence)
- There will be a reduction of Southwest mountain snowpack during February through May from 2001 through 2100, mostly because of the effects of warmer temperature. (high confidence)
- Substantial parts of the Southwest region will experience reductions in runoff and streamflow from the middle to the end of the twenty-first century. (medium-high confidence)

6.1 Global Climate Models: Statistical and Dynamical Downscaling

Global climate models (GCMs) are the fundamental drivers of regional climate-change projections (IPCC 2007). GCMs allow us to characterize changes in atmospheric circulation associated with human causes at global and continental scales. However, because of the planetary scope of the GCMs, their resolution, or level of detail, is somewhat coarse. A typical GCM grid spacing is about 62 miles (100 km) or greater, which is inadequate for creating projections and evaluating impacts of climate change at a regional scale. Thus, a “downscaling” procedure is needed to provide finer spatial detail of the model results.

Downscaling is done in two ways—statistical (or empirical) downscaling and dynamical downscaling—each with its inherent strengths and weaknesses. Statistical downscaling relates historical observations of local variables to large-scale measures. For climate modeling, this means taking the observed relationship of atmospheric circulation and regional-scale surface data of interest (temperature and precipitation) and applying those empirical relationships to GCM data for some future period (Wilby et al. 2004; Maurer et al. 2010). Many of the results shown here, involving projected temperature and precipitation, are based upon a “bias correction and spatial downscaling”

(BCSD) method (Maurer et al. 2010).ⁱ “Bias” is a statistical term reflecting systematic error. The main advantage of statistical downscaling is that it is computationally simple, so a relatively large number of GCMs and greenhouse gas emission scenarios may be considered for a more robust characterization of statistical uncertainty (Maurer et al. 2010).ⁱⁱ

In contrast, dynamical downscaling produces climate information by use of a limited-area, regional climate model (RCM) driven by the output from a global climate model (Mearns et al. 2003; Laprise et al. 2008). Dynamical RCMs, similar to GCMs, are numerical representations of the governing set of equations that describe the climate system and its evolution through time over a particular region. Though use of a physically based process model at a grid spacing of tens (rather than hundreds) of kilometers is substantially more computationally expensive, the method has two advantages over statistical downscaling. Climate stationarity (the concept that past climatic patterns are a reasonable representation of those in the future) is not assumed and the influence of complex terrain on the climate of the western United States is better represented (Mearns et al. 2003), improving the simulation of precipitation from winter storms (Ikeda et al. 2010) and thunderstorms during the summer monsoon (Gutzler et al. 2005). However, because of their cost, long runs (lengthy computer processing) of regional climate simulations generally are not undertaken. In addition, each regional model contains some degree of bias, so statistical adjustments are almost always required. In other words, regardless of whether statistical or dynamical downscaling is pursued, bias-correction of GCM or GCM-RCM output is a necessary part of the process.

In this chapter, we use the “variable infiltration capacity” (VIC) model (Liang et al. 1994) to derive land-surface hydrological variables that are consistent with the downscaled forcing data.ⁱⁱⁱ The VIC model has been applied in many studies of hydrologic impacts of climate variability and change (e.g. Wood et al. 2004; Das et al. 2009).

6.2 Climate Scenarios

Following the lead of the U.S. National Climate Assessment, the *Special Report on Emissions Scenarios* A2 (“high emissions”) and B1 (“low emissions”) scenarios (IPCC 2007) are employed here (see endnote iii in Chapter 2).

The choice of the high (A2) and low (B1) emissions scenarios was also guided by the need to span a range of GHG emissions and the availability of a reasonably large number of GCM simulations. GCMs, to varying degrees, capture average recent historical climate and a statistical representation of its variability over the Southwest (Ruff, Kushnir, and Seager 2012) and to some extent key regions such as the tropical Pacific that are known to drive important climate variations in the Southwest region (Dai 2006; IPCC 2007; Cayan et al. 2009). Many applications employ multiple model simulations, made for one or more GHG emissions scenario using one or more GCMs, which are generally referred to as an ensemble. Beyond this, however, it has been shown (Pierce et al. 2009; Santer et al. 2009) that a model’s performance in simulating characteristics of observed climate is not a very useful measure of how well it will simulate future climate under climate change. Because of this, it is better to draw upon a number of simulations to construct a possible distribution of climate change; i.e., it is important to consider results from several climate models rather than to rely on just a few.

6.3 Data Sources

Projected climate for the *Assessment of Climate Change in the Southwest United States* is based on a series of GCM and downscaled projection data sets. A set of CMIP3^{iv} GCM outputs, from fifteen GCMs (used in an initial set of experiments) and sixteen GCMs (used in later experiments) that were identified in the 2009 NCA report, provided a core set of thirty and thirty-two climate simulations, respectively. Each GCM simulated one high- and one low-emissions scenario. Only one simulation for each individual GCM-emissions scenario pairing was included. The GCMs provide historical simulations in addition to projected twenty-first-century climate simulations based on the high- and low-emissions scenarios.

Statistical downscaled monthly temperature and precipitation data from the sixteen GCMs using the BCSD method were employed. These data are at a horizontal resolution of 1/8° (roughly 7.5-mile [12-km] resolution), covering the period of 1950–2099 (Maurer, Brekke et al. 2007; Gangopadhyay et al. 2011).

Dynamical downscaled simulations from the multi-institutional North American Regional Climate Change Assessment Program (NARCCAP; Mearns et al. 2009) were used. At this time, there are nine high-emissions simulations available using different combinations of a regional climate model driven by a global climate model. Each simulation includes the periods of 1971–2000 and 2041–2070 for the high-emissions scenario only, and is at a horizontal resolution of approximately 31 miles (50 km).

Peer-reviewed and publicly available hydrologic projections (Gangopadhyay et al. 2011) are associated with the same BCSD CMIP3 climate projections that are supporting evaluations in this chapter. Hydrologic simulations using the VIC model from each of the sixteen historical BCSD simulations, sixteen high-emissions BCSD simulations, and sixteen low-emissions BCSD simulations were employed.

6.4 Temperature Projections

There is high confidence that climate will warm substantially over the twenty-first century, as all of the projected GCM and associated downscaled simulations exhibit progressive warming over the Southwest United States. Within the modeled historical simulations, the model warming begins to become distinguished from the range of natural variability in the 1970s; similar warming is also found in observed records and appears, partially, to be a response to the effects of GHG increases (Barnett et al. 2008; Bonfils et al. 2008). Concerning the projected climate, in the early part of the twenty-first century, the warming produced by the high-emissions scenario is not much greater than that of the low-emissions scenario; there is considerable overlap between the high- and low-emissions scenario results. But by the mid-2000s, as GHG concentrations under the high-emissions scenario become considerably higher than those in the low-emissions scenario, warming in the high-emissions simulations becomes increasingly greater than those from the low-emissions scenario. The projected rate of warming is substantially greater than the historical rates estimated from observed temperature records in California (Bonfils et al. 2008).

Maps showing the sixteen CMIP3 ensemble mean annual temperature changes for three future time periods (2035, 2055, 2085) and two emissions scenarios (high and low)

are shown in Figure 6.1. The three periods show successively higher temperatures than the model-simulated historical mean for 1971–2000. Spatial variations are relatively small, especially for the low-emissions scenario. Changes along the coastal zone are noticeably smaller than inland areas (see also Cayan et al. 2009; Pierce et al. 2012). Also, the warming tends to be slightly greater in the north, especially in the states of Nevada, Utah, and Colorado. Warming increases over time, and also increases between the high- and low-emissions scenarios for each respective period as shown in the thirty-year early-, mid-, and late-twenty-first century plots in Figure 6.2 for the aggregated six-state region that defines the Southwest. Figure 6.3 shows the mean seasonal changes for each future time period for the high-emissions scenario, averaged over the entire Southwest region for fifteen CMIP3 models. For the low-emissions scenario, the amount of annual warming ranges between 1°F and 3°F (0.6°C to 1.7°C) for the period, 2021–2050; over 1°F

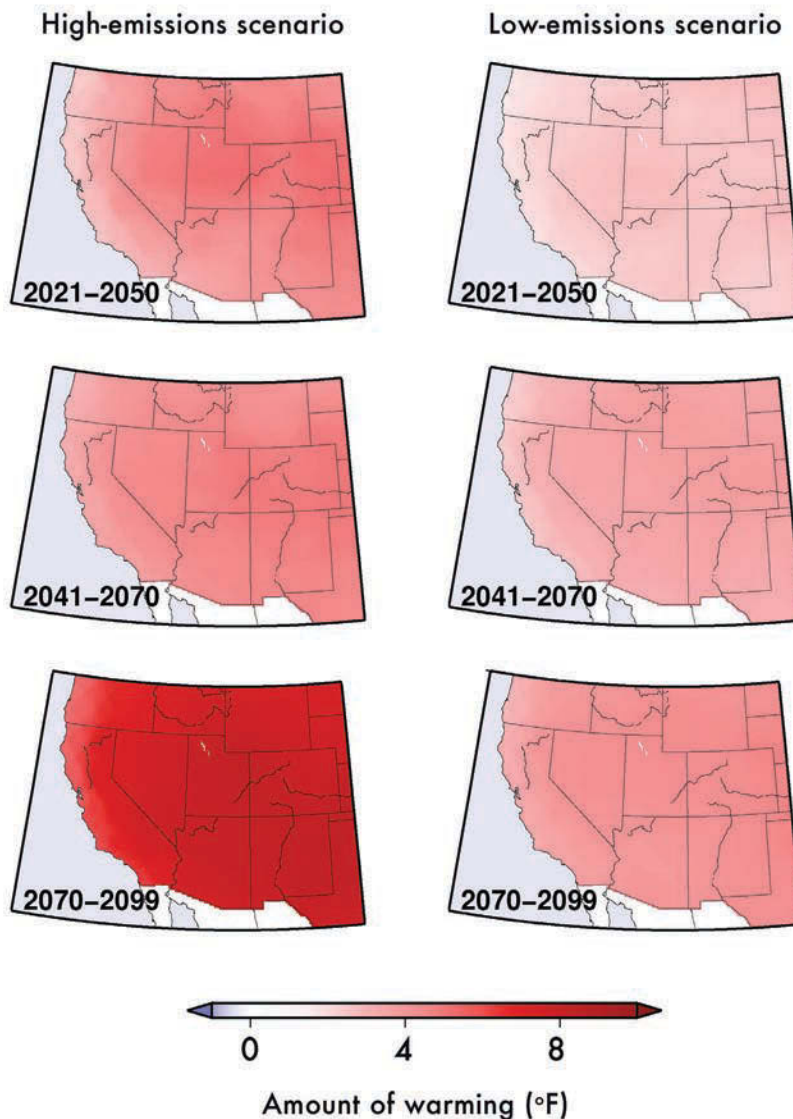


Figure 6.1 Projected temperature changes for the high (A2) and low (B1) GHG emission scenario models. Annual temperature change (°F) from historical (1971–2000) for early- (2021–2050; top), mid- (2041–2070; middle) and late- (2070–2099; bottom) twenty-first century periods. Results are the average of the sixteen statistically downscaled CMIP3 climate models. Source: Nakićenović and Swart (2000), Mearns et al. (2009).

to 4°F (0.6°C to 2.2°C) for 2041–2070; and 2°F to 6°F (1.1°C to 3.3°C) for 2070–2099. For the high-emissions scenario, values range slightly higher, from about 2°F to 4°F (1.1°C to 2.2°C) for 2021–2050; 2°F to 6°F (1.1°C to 3.3°C) for 2041–2070; and are much higher, a 5°F to 9°F (2.8°C to 5°C) range, by 2070–2099. For 2055, the average temperature change simulated by the NARCCAP models (4.5°F, or 2.5°C) is close to the mean of the CMIP3 GCMs for the high-emissions scenario.

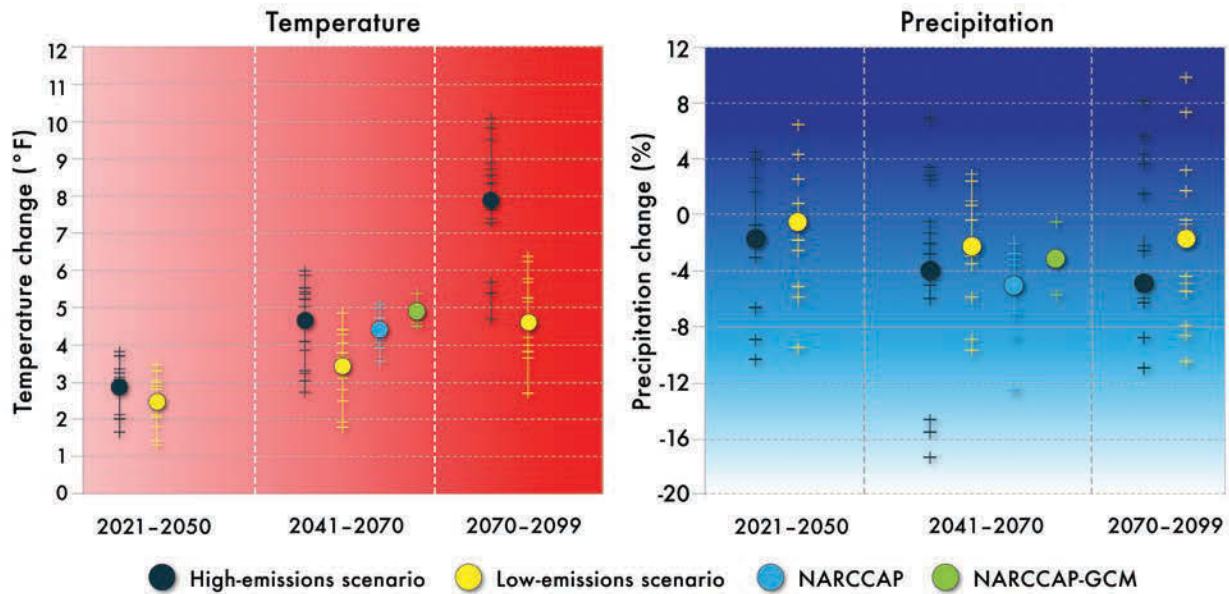


Figure 6.2 Mean annual temperature changes (°F; left) and precipitation changes (%; right) for early-, mid- and late-twenty-first-century time periods. Temperature changes and precipitation changes are with respect to the simulations' reference period of 1971–2000 for 15 CMIP3 models, averaged over the entire Southwest region for the high (A2) and low (B1) emissions scenarios. Also shown are results for the NARCCAP simulations for 2041–2070 and the four GCMs used in the NARCCAP experiment (A2 only). The small plus signs are values for each individual model and the circles depict the overall means. Source: Nakicerońić and Swart (2000), Mearns et al. (2009).

The warming, as it emerges from the variability within and across model simulations, is shown for each of three subregions in the Southwest by the ensemble time series in Figure 6.4. Temperature increases are largest in summer, with means around 3.5°F (1.9°C) in 2021–2050, 5.5°F (3.1°C) in 2041–2070, and 9°F (5°C) in 2070–2099. The least warming is in winter, starting at 2.5°F (1.4°C) in 2021–2050 and building to almost 7°F (3.9°C) in 2070–2099. However, it is important to note that differences between individual model temperature changes are relatively large. Within a given emissions scenario, differences in the resultant mean temperature of the simulations can be attributed to differences in the models (for example, the way they represent and calculate key physical processes) and from differences across simulations resulting from the inherent

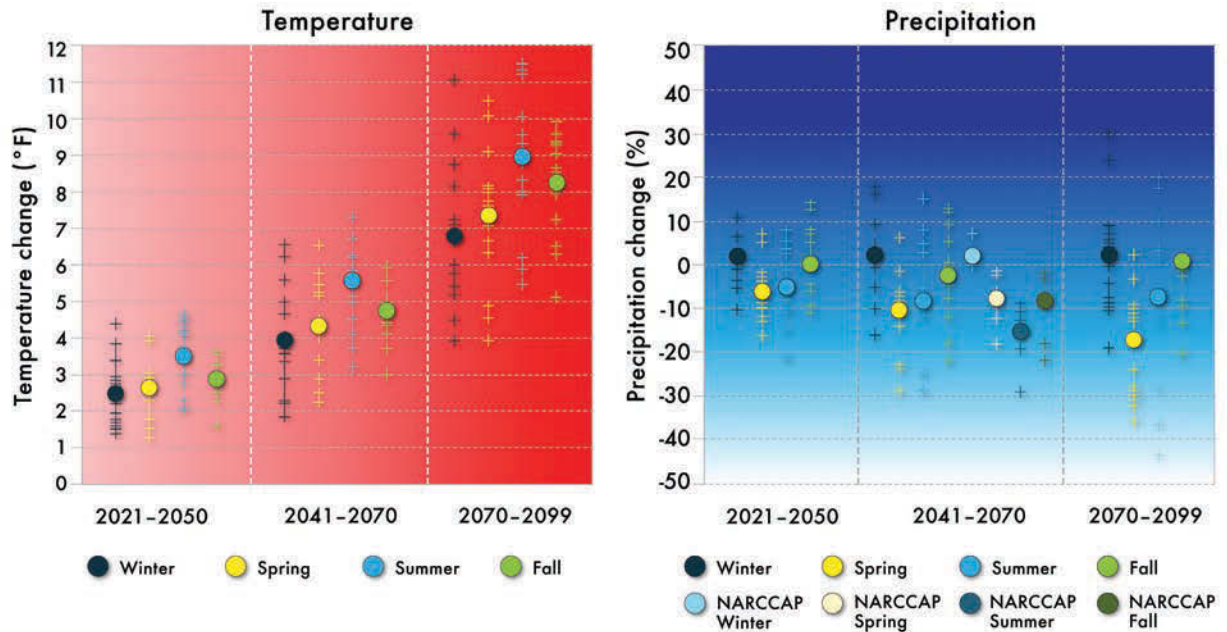


Figure 6.3 Projected change in average seasonal temperatures (°F, left) and precipitation (% change, right) for the Southwest region for the high-emissions (A2) scenario. A fifteen-model average of mean seasonal temperature and precipitation changes for early-, mid-, and late-twenty-first century with respect to the simulations' reference period of 1971–2000. Changes in precipitation also show the averaged 2041–2070 NARCCAP four global climate model simulations. The seasons are December–February (winter), March–May (spring), June–August (summer), and September–November (fall). Plus signs are projected values for each individual model and circles depict overall means. Source: Mearns et al. (2009).

variability of shorter-period climate fluctuations (Hawkins and Sutton 2009). The magnitude of the differences between models using the same emissions scenario is large compared to the difference in the change between seasons and to the difference between high- and low-emissions scenarios, and is comparable to that of the mean differences between the projections for the early- and late-twenty-first century.

6.5 Projections of Other Temperature Variables

The projected length of the annual freeze-free season increases across the region, which historically has exhibited a freeze-free season ranging from 50 to 300 days, depending on location (Figure 6.5, top). By the mid-twenty-first century (Figure 6.5, bottom, from NARCCAP simulations), the entire region exhibits increases of at least 17 additional freeze-free days, excepting parts of the California coast, which show increases of 10 to 17 days. The largest increases, more than 38 days, are in the interior far West. The freeze-free season in eastern parts of Colorado and New Mexico increases by 17 to 24 days, while in some areas along the Rocky Mountains it increases up to 30 days.

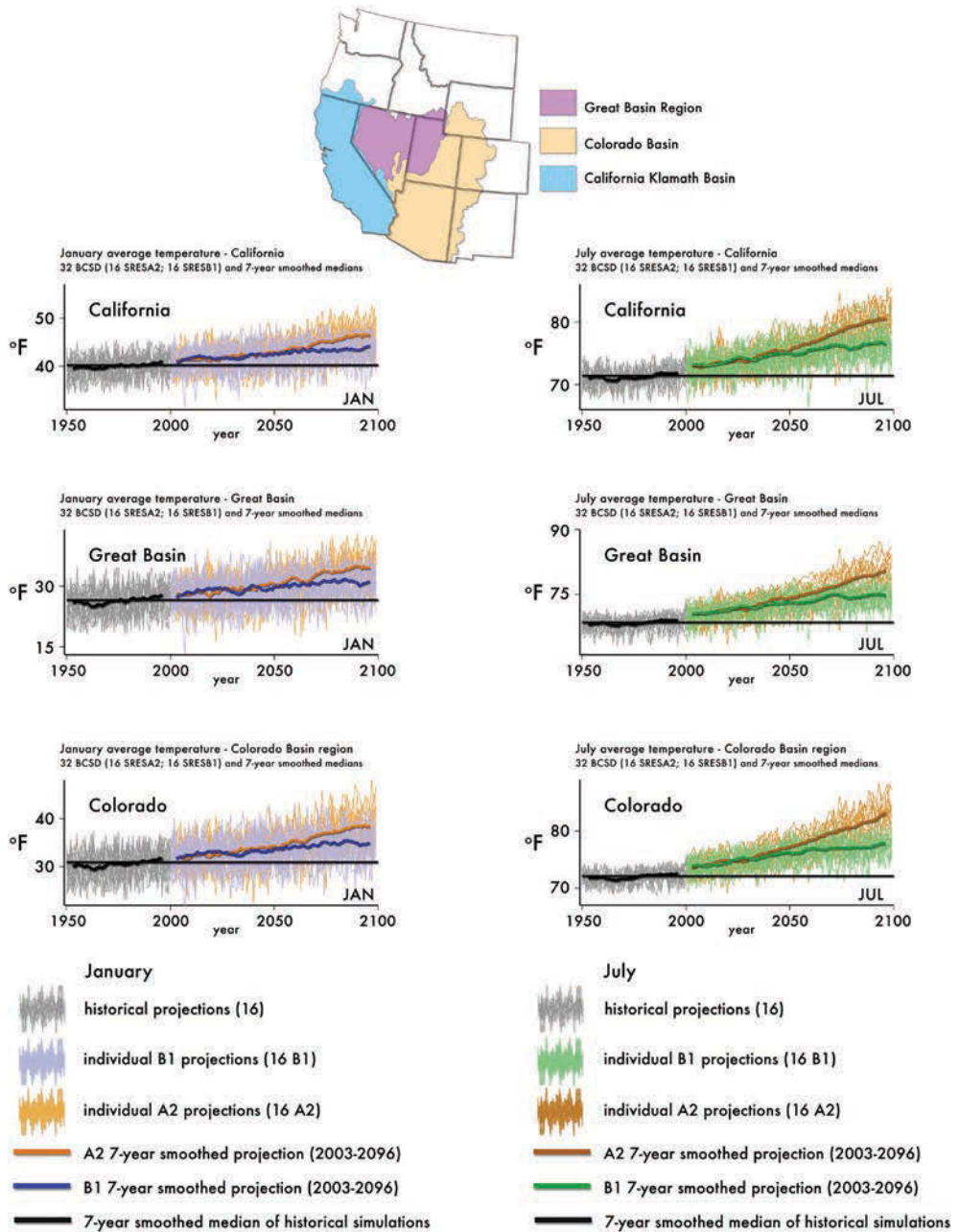


Figure 6.4 January (left) and July (right) BCS D average temperature for California (top), the Great Basin (middle), and Colorado (bottom). The maps show the three regions over which the temperatures were averaged. Source: Bias Corrected and Downscaled World Climate Research Programme's CMIP3 Climate Projections archive at http://gdo-dcp.ucllnl.org/downscaled_cmip3_projections/#Projections:%20Complete%20Archives.

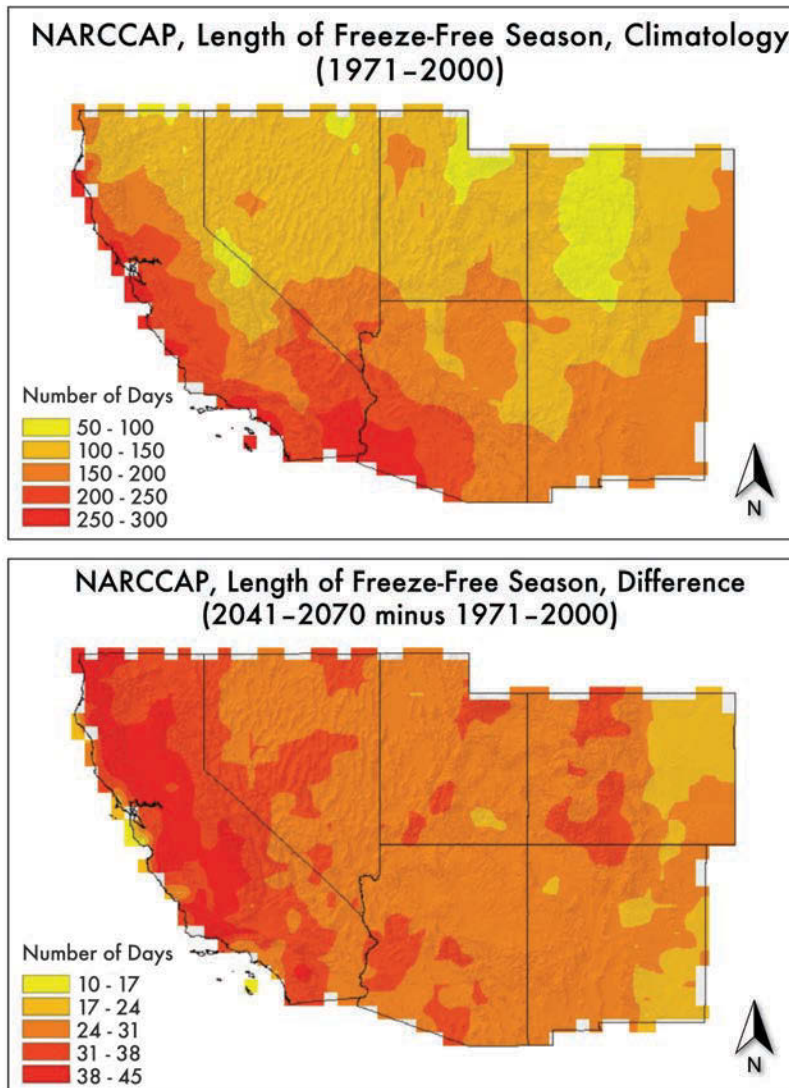


Figure 6.5 NARCCAP multi-model mean change in the length of the freeze-free season between 2041–2070 and 1971–2000 (top) and simulated NARCCAP climatology of the length of the freeze-free season (bottom). Source: Mearns et al. (2009).

Heating degree days (a measurement that reflects the amount of energy needed to heat a home or structure) decrease substantially. In general, by the mid-twenty-first century as gauged from the mean of NARCCAP simulations, the entire region is projected to experience a decrease of at least 500 heating degree days per year, using a heating degree day baseline of 65°F.^v The largest changes occur in higher-elevation areas, where the decreases are up to 1,900 heating degree days. Areas along the coast, along with southern Arizona, are projected to experience the smallest decreases in heating degree days per year.

On the other hand, cooling degree days increase over the entire Southwest region, with the warmest areas showing the largest increases and vice versa for the coolest areas. The hottest areas, such as Southern California and southern Arizona, are simulated to have the largest increase of cooling degree days per year, up to 1,000, using a 65°F

baseline. Areas east of the Rocky Mountains, as well as the California coast, show increases of 400 to 800 cooling degree days per year. Areas with the highest elevations, including the Rocky Mountains and the Sierra Nevada, have the smallest simulated increases, around 200 days or fewer. Cooling and heating requirements become acute during extreme conditions that fall into the tail of the temperature distribution—heat waves and cool outbreaks—whose future occurrences and intensity are affected by the underlying changes in the center of the distribution as described in Chapter 7.

6.6 Precipitation Projections

The precipitation climatology in the Southwest is marked by a large amount of spatial and temporal variability. Observed variability over time in parts of the Southwest, as scaled by mean precipitation, is greater than that in other regions of the United States (Dettinger et al. 2011), from few-day events (see Chapter 7) to scales of months, years, and decades (Cook et al. 2004; Woodhouse et al. 2010). The climate-model-projected simulations indicate that a high degree of variability of annual precipitation will continue during the coming century, as illustrated by the ensemble time series of annual total precipitation in inches shown in Figure 6.6. This suggests that the Southwest will remain susceptible to unusually wet spells and, on the other hand, will remain prone to occasional drought episodes.

To some degree, the model simulations also contain trends over the twenty-first century, as presented in Table 6.1. It is emphasized that these results have medium-low confidence, however, because the trends are generally small in comparison to the high level of shorter-period variability and the considerable variability that occurs among model simulations. As with the temperature projections, the difference in mean precipitation over a given epoch between simulations is due to internal variability, differences between model formations, and between emissions scenarios (Hawkins and Sutton 2009). The distribution of the CMIP3 multi-model median changes in annual precipitation, as a fraction of the modeled historical (1971–2000) annual mean, is shown in Figure 6.7 for the three future periods: 2021–2050 (referred to as “2035”), 2041–2070 (or “2055”), and 2070–2099 (or “2085”) and for the low-emissions and high-emissions scenarios. Generally, the median changes shift from drier conditions (than historical climatology) in the south to somewhat wetter in the north. In the high-emissions simulations these changes increase in magnitude through the twenty-first century, but in the low-emissions scenario the differences over time are not as great and peak near the mid-twenty-first century, as seen in Figure 6.7 and at the right in Figure 6.2. The largest north-south percentage differences are for the high-emissions scenario in 2085, varying from an increase of 2% in the far north of the Southwest region to a decrease of 12% in the far south of the Southwest. The smallest difference occurs for the high-emissions scenario in 2035, with increases of 2% in the Nevada-Utah area, and a decrease of about 4% to 6% in areas such as Colorado, New Mexico, and California. However, in the high-emissions scenario in the late twenty-first century, weak increases are found in median precipitation in southeastern California and southern Nevada.

Figure 6.2, right panel, shows the mean annual changes in precipitation for each future time period and both emissions scenarios, averaged over the entire Southwest region for fifteen CMIP3 models. In addition, averages for the nine NARCCAP simulations and

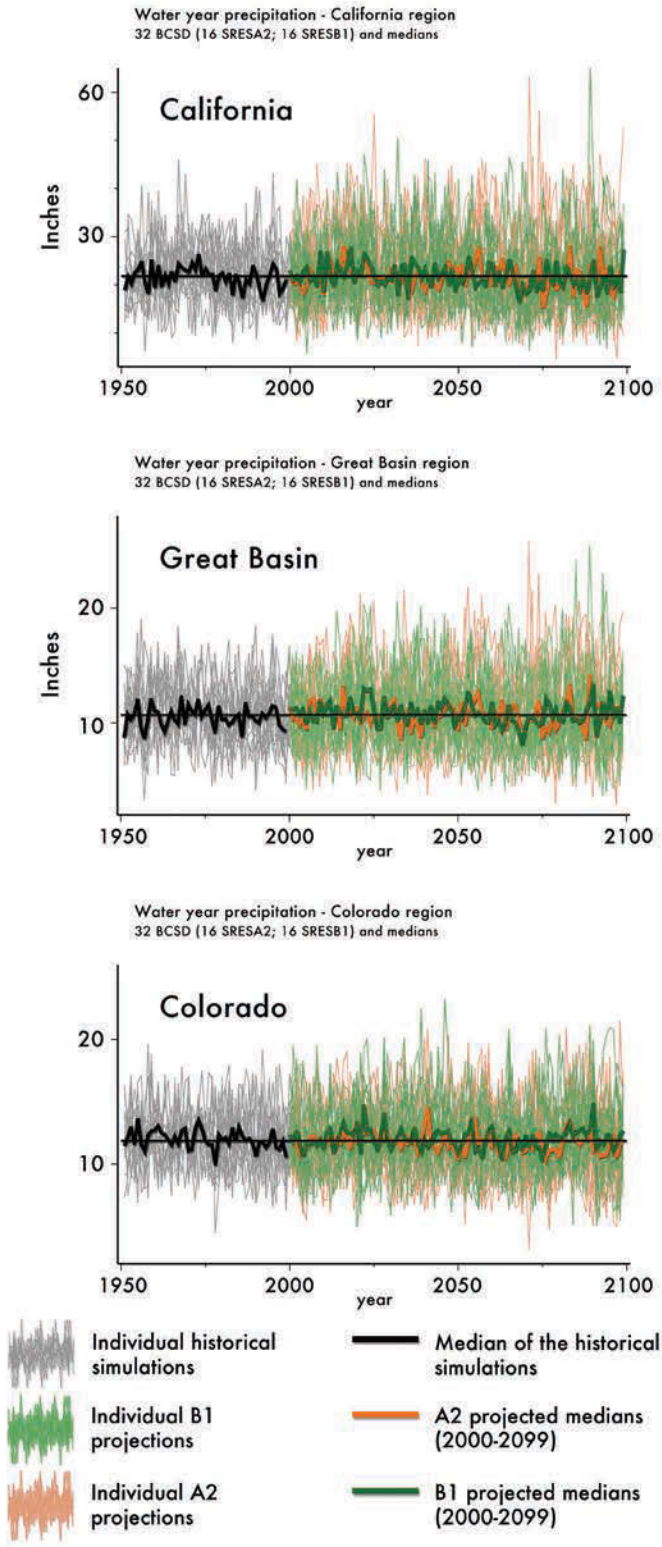


Figure 6.6 Water year precipitation (in inches) averaged over California (top), Great Basin (middle) and Colorado (bottom). Source: Bias Corrected and Downscaled World Climate Research Programme's CMIP3 Climate Projections archive at http://gdo-dcp.ucllnl.org/downscaled_cmip3_projections/#Projections:%20Complete%20Archives.

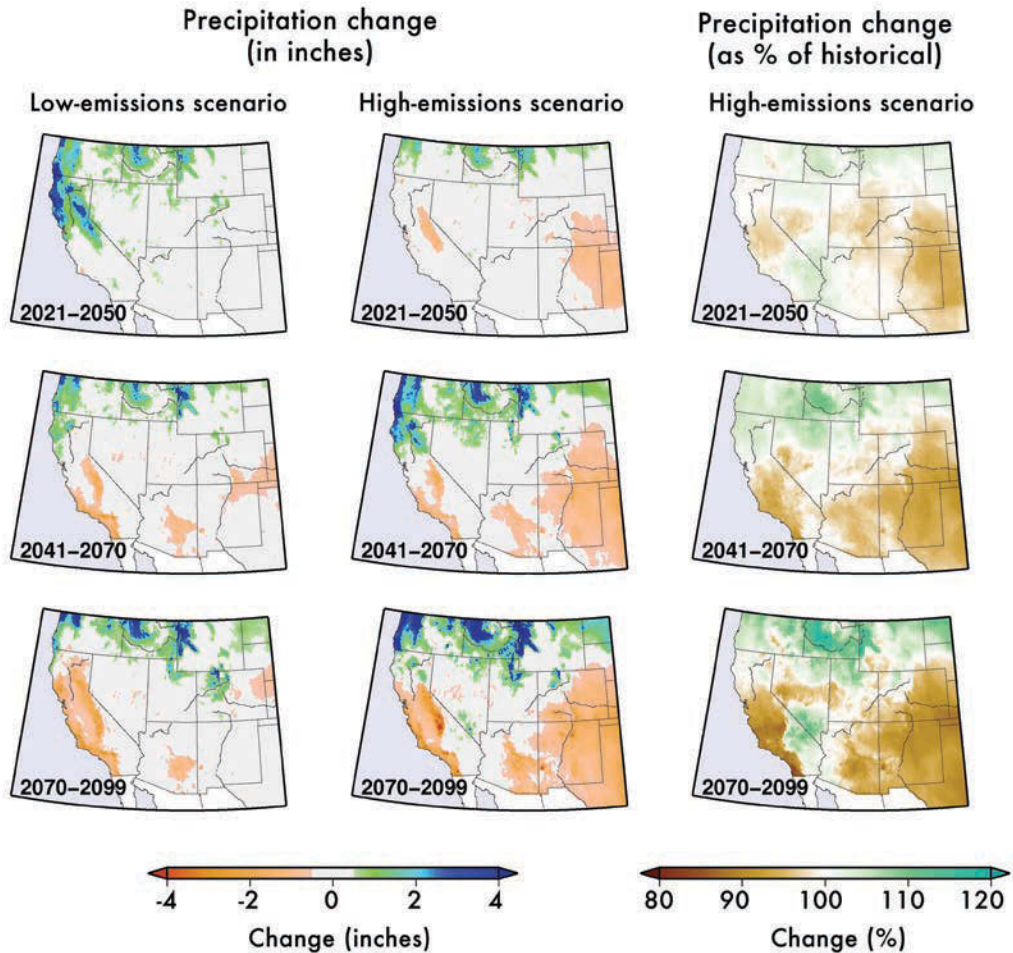


Figure 6.7 Annual precipitation change (in inches) from the historical simulation for the low-emissions scenario (left), the high-emissions scenario (middle), and percentage of historical simulation compared to the high-emissions scenario (right). Early- (2021–2050), mid- (2041–2070) and late- (2070–2099) twenty-first century periods shown in top, middle and bottom panels. Values shown are the median of sixteen simulations downscaled via BCS. Source: Bias Corrected and Downscaled World Climate Research Programme’s CMIP3 Climate Projections archive at http://gdo-dcp.ucllnl.org/downscaled_cmip3_projections/#Projections:%20Complete%20Archives.

the four GCMs used in the NARCCAP experiment are shown for 2055 (high-emissions scenario only). All the mean changes are negative, although the values are rather small overall. For the high-emissions scenario, the CMIP3 models project average decreases of around 2% in 2035, 4% by 2055, and about 5% by 2085. The decreases for the low-emissions scenario are only slightly smaller; in 2085 the decrease is 2%, compared to 5% for high-emissions. The mean of the NARCCAP simulations is more negative than the mean of the CMIP3 GCMs or the mean of the four GCMs used in the NARCCAP experiment, although the differences are small. The range of individual model changes is large compared to the differences in the ensemble means, as also illustrated by the spread of

changes shown in Table 6.1. In fact, for all three future periods and for the two scenarios, the individual model range is larger than the differences in the CMIP3 ensemble mean changes, relative to the historical mean precipitation.

The distribution of changes in the Southwest region's mean annual precipitation for each future time period and both emissions scenarios across the fifteen CMIP3 models is shown in Figure 6.2, right panel, and in Table 6.1, which also shows the distribution of the NARCCAP simulations (for 2055, high-emissions scenario only) for comparison. For all periods and both scenarios, the CMIP3 model simulations include both increases and decreases in precipitation. For the region as a whole, most of the median values are negative, but not by much, with change values having magnitudes of 3.1% or less. The range of changes is between 15% and 30%. For example, in the high-emissions scenario, the precipitation change for 2055 varies from a low of -17% to a high of +7%. The NARCCAP range of changes varies from -13% to -2%.

Table 6.1 Distribution of changes in mean annual precipitation (%) for the Southwest region for the 15 CMIP3 models

Scenario	Period	Low	25%ile	Median	75%ile	High
A2	2021-2050	-10	-3	-2	2	5
	2041-2070	-17	-6	-3	1	7
	2070-2099	-20	-10	-3	3	8
	NARCCAP	-13	-7	-3	-3	-2
B1	2021-2050	-10	-2	1	2	6
	2041-2070	-10	-3	-2	0	3
	2070-2099	-10	-5	-1	1	10

Annual precipitation changes over individual regions are stronger or weaker than the aggregate Southwest, as exhibited by the median of the ensemble high-emissions and low-emissions simulations for California, the Great Basin, and the Colorado Basin regions in Figure 6.6. These reinforce the evidence from the mapped median changes in Figure 6.7, showing that the California region exhibits the greatest reduction in precipitation, while the Colorado Basin remains nearly the same as historical levels. The ensemble swarms in Figure 6.6 emphasize the importance of individual wet years in affecting longer term climatological values; at least for a few models, the wettest years grow wetter during the last half of the twenty-first century.

Considering the Southwest as a whole, a majority of the models contain different levels and even directions of change in different seasons, as shown in Table 6.2 and Figure 6.3, right panel. These include increases in winter precipitation, while for the other three seasons, most of the models simulate decreases. In the spring, all but one model

simulate decreases. In both the summer and fall, a few models produced sizeable increases in precipitation. In the low-emissions scenario, the range of changes is generally smaller, with a tendency toward somewhat wetter conditions. For example, a majority of the low-emissions models simulate wetter conditions, as compared to the drier majority for the high-emissions scenario. A central feature of the results shown in Table 6.2 is the tendency for greatest precipitation reductions in spring months, albeit with large uncertainty in the seasonal changes (as expressed by the range of results across the ensemble of model simulations).

Table 6.2 Distribution of changes in mean seasonal precipitation (%) for the Southwest region for the 15 CMIP3 models

Scenario	Period	Season	Low	25%ile	Median	75%ile	High
A2	2070-2099	DJF	-19	-8	3	8	30
		MAM	-36	-29	-12	-10	2
		JJA	-44	-13	-9	3	20
		SON	-21	-8	-1	0	38
B1	2070-2099	DJF	-12	-6	2	5	17
		MAM	-27	-9	-7	-1	11
		JJA	-16	-7	0	3	18
		SON	-24	-4	-1	6	13

6.7 Atmospheric Circulation Changes

Climate changes in the Southwest are governed overwhelmingly by global influences. The IPCC Fourth Assessment Report indicated that several climate models project that the mid-latitude storm tracks in both the Southern and Northern Hemispheres will migrate poleward over the twenty-first century (e.g. Meehl et al. 2007). This result was reinforced by analyses by Salathé (2006) and Cayan et al. (2009), who showed a northward shift in the North Pacific winter storm track over the mid- and late-twenty-first century. This result is consistent with the findings of Favre and Gershunov (2009), who examined paths of mid-latitude cyclones and anticyclones^{vi} in the North Pacific impinging on the North American West Coast in observations and in the CNRM-CM3 model^{vii} high-emissions projection. Wintertime statistics of these trajectories indicate that the flow pattern will become less stormy in the Gulf of Alaska, with more northerly flow along the West Coast of North America. This projected trend is on par with interannual variability in this region and indicates future conditions somewhat reminiscent of today's La Niña phase of the El Niño-Southern Oscillation (ENSO) and negative-phase

Pacific Decadal Oscillation (PDO) winters. These projected circulation changes would result in less frequent winter precipitation in the Southwest United States and northwestern Mexico, and more frequent, albeit less intense, cold outbreaks moderating average wintertime warming, especially in California's low-lying valleys and east of the Front Range of the Rocky Mountains (see Chapter 7).

The shift of the mid-latitude northeastern Pacific storm track poleward may be a result of uneven warming over the earth's surface. Warming is projected to be lower at the low latitudes than the high latitudes, causing a diminished gradient of temperature from the equator to the North and South Poles (Lambert 1995; Lambert and Fyfe 2006; IPCC 2007). In a warming atmosphere, the models also predict increasing humidity. Enhanced evaporation from the ocean's surface and the resulting heating of the atmosphere from condensation of water vapor aloft could reinforce the deepest cyclones, making deep low pressure systems (cyclonic storms) more numerous while moderate events decline in frequency (Lambert 1995; Lambert and Fyfe 2006).

The storm track displacement is also consistent with the projected enhancement and poleward extension of the large descending limb of the tropical atmospheric circulation—the Hadley Cell, which impels the trade winds and jet stream in the tropics and subtropics (see, for example, Lu, Vecchi, and Reichler 2007). The enhancement and broadening of subsiding air in the subtropics and low middle latitudes of the eastern North Pacific could also result in an increase and seasonal expansion of the low-level coastal clouds, the “marine layer” along the California coast, especially in spring and summer. This important potential impact on coastal climate has so far not been investigated.

6.8 North American Monsoon

Representing the North American monsoon (see Chapter 4) in an atmospheric model is extremely challenging because it is governed by multiple factors at different spatial and temporal scales (Douglas and Englehart 2007; Bieda et al. 2009). Most important, the initiation of convection over mountains during the day and thunderstorm organization and growth must be appropriately addressed (Janowiak et al. 2007; Lang et al. 2007; Nesbitt, Gochis, and Lang 2008). GCMs cannot resolve the North American monsoon as a distinct climatological feature because they cannot resolve several key regional processes (Liang et al. 2008; Dominguez, Cañon, and Valdes 2009). Dynamical downscaling using RCMs (at a grid spacing of tens of kilometers) has simulated well at least the start of the convective process over mountains and improved the climatology of monsoon precipitation (Gutzler et al. 2005; Castro, Pielke, and Adegoké 2007). Very high resolution (1.2 mile, or 2-km grid spacing or less) is required to simulate the *evolution* of organized convection so that individual thunderstorms can be explicitly represented (Gao, Li, and Sorooshian 2007). Interannual variability of monsoon precipitation in the Southwest United States is related in part to ENSO and PDO variability (Dominguez, Kumar, and Vivoni 2008). How this natural variability may potentially change in the future is not clear in the GCMs and is a source of large uncertainty (Castro et al. 2007). The evolving pattern of sea-surface temperature is generally important for models to properly simulate key changes in surface temperature and precipitation on a regional scale (Barsugli, Shin, and Sardeshmukh 2006). Moreover, enhanced subsidence of air

in the subtropical region (as described in Lu, Vecchi, and Reichler 2007) can potentially impact convection and therefore moderate the monsoon, but this possible mechanism of monsoonal change has so far been unexplored. In general, future expectations of the North American monsoon suffer from uncertainties currently common to monsoon systems around the world.

Figure 6.8 shows the simulated changes in warm-season (June through September) temperature and precipitation in the NARCCAP high-emissions simulations, shaded according to the level of model agreement. The ensemble mean change in model temperatures shows summer warming that ranges between +2°F and +6°F throughout most of the western United States by the middle of the twenty-first century (2041–2069), with the largest temperature increases in the central Rocky Mountains. Precipitation is projected to decrease overall in the Southwest by about 10% to 20%, consistent with an overall drying trend in subtropical regions. This projected precipitation decrease is relatively smaller in eastern Arizona and western New Mexico, with relatively weaker agreement among the individual models. Though NARCCAP models strongly agree as to the amount of warming during the warm season, the weak level of consensus about changes in the monsoon circulation reflects the enormous challenges of representing the monsoon in an atmospheric model. In summary, how monsoon precipitation may change is not yet clear, especially in those areas where monsoon precipitation accounts for a greater proportion of total annual precipitation.

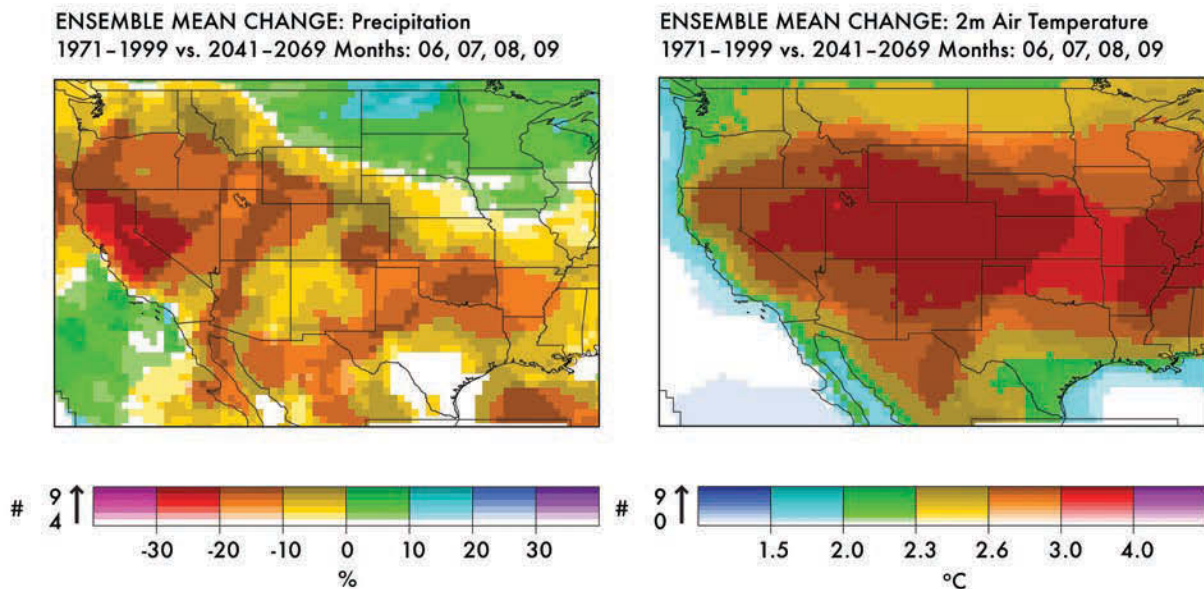


Figure 6.8 NARCCAP precipitation and temperature difference, June–September, 2041–2069 relative to simulated historical means 1971–1999. The degree of change is indicated by the color, whereas the degree of agreement among the nine RCMs is indicated by the intensity of the color. For precipitation (left), the color intensity shows the agreement among the RCMs on the direction of change (i.e., positive or negative percent change in future precipitation); for temperature (right), the color intensity shows agreement among the RCMs on areas where future temperature is projected to be at least 2°C (3.6°F) higher than the 1971–1999 average. Source: Mearns et al. (2009).

6.9 Changes in Precipitation-related Measures

The escalating effect of warming, coupled with a tendency in parts of the Southwest toward annual precipitation decreases, would amplify recent observed trends of lower spring snowpack across much of the western United States (Mote et al. 2005; Knowles, Dettinger, and Cayan 2006; Pierce et al. 2008). Additionally, the Southwest straddles both a region to the north where precipitation is projected to increase and a region to the south where precipitation is projected to decrease—as shown by a consensus of global model simulations (IPCC 2007; Seager and Vecchi 2010). The GCM projections, down-scaled and run through the VIC hydrological model, show changes in hydrological measures that are consistent with the warming trend. They indicate a marked reduction in spring snow accumulation in mountain watersheds across the Southwestern United States (Figure 6.9 top panel) that becomes more pronounced over the decades of the twenty-first century. The relatively gradual decline for the California, Colorado, and Rio Grande basins shown in Figure 6.10 (top row) is consistent with several other studies (e.g. Knowles and Cayan 2002; Christensen and Lettenmaier 2007; Ray et al. 2008; Cayan et al. 2009; Das et al. 2009; Wi et al. 2012). More rain and less snow, earlier snowmelt, and, to some extent, drying tendencies cause a reduction in late-spring and summer runoff (Figure 6.9, middle panel, and 6.10, middle row). Together these effects, along with increases in evaporation, result in lower soil moisture by early summer (Figure 6.9, bottom panel, and 6.10, bottom row).

Recent studies have projected Colorado River flows to show possible reductions from climate-change impacts, ranging from about -5% to about -20% by mid-century (Hoerling and Eischeid 2007; Das et al. 2011; Reclamation 2011a; Vano, Das, and Lettenmaier 2012). Changes in streamflow are driven by changes in precipitation and also by increases in temperature. Recent estimates, from several hydrological models, suggest reductions in annual Colorado River flow at Lees Ferry, Arizona, which is the location established by the Colorado River Compact in 1922 as the dividing point between the Upper Colorado River Basin and the Lower Colorado River Basin. Estimates of the reductions in Colorado River flow range from approximately 3% to 16% decrease per 1°F (0.6°C) warming and a reduction of 1% to 2% of flow per 1% reduction of precipitation (Hoerling et al. 2009; Reclamation 2011b; Vano, Das, and Lettenmaier 2012). As estimated by the VIC hydrological model, runoff and streamflow are more sensitive to warming in the Colorado Basin than in the Columbia River watershed and are much greater than in the northern and southern drainages of the Sierra Nevada in California (Das et al. 2011). Figure 6.11, based on the ensemble of sixteen VIC simulations under the high-emissions scenario, shows the median tendency for reductions in total annual runoff over the Southwest in the mid-twenty-first century. Over the Colorado Basin, the composite of simulations from the VIC simulations exhibits reductions of runoff of approximately 5% to 18% by the middle portion of the twenty-first century, consistent with the estimates described above.

The early twenty-first-century drought in the Southwest (see Chapters 4 and 5) underscores that the Southwest climate is prone to dry spells. Such droughts have a tendency to take on large areal footprints, although both observations and climate model simulations indicate different degrees of dryness in California, the Great Basin, and the Colorado Basin. As quantified by the VIC hydrological model, the most extreme drought

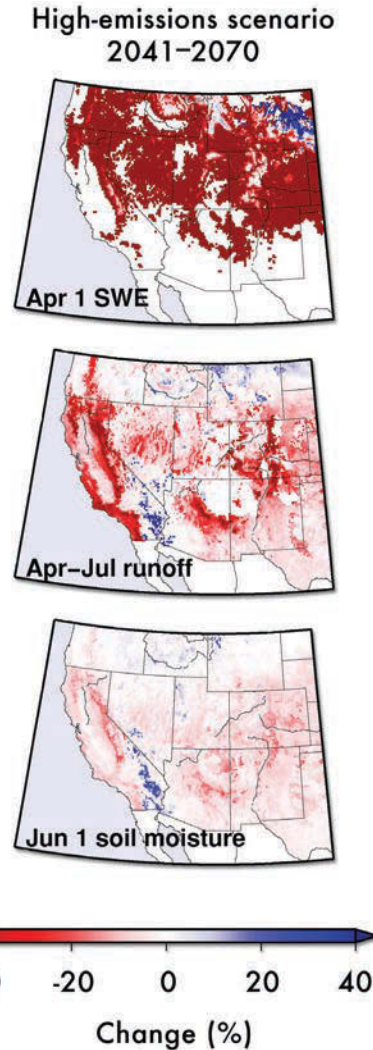


Figure 6.9 Predicted changes in the water cycle.

Mid-century (2041–2070) percent changes from the simulated historical median values from 1971–2000 for April 1 snow water equivalent (SWE, top), April–July runoff (middle) and June 1 soil moisture content (bottom), as obtained from median of sixteen VIC simulations under the high-emissions (A2) scenario. Source: Bias Corrected and Downscaled World Climate Research Programme’s CMIP3 Climate Projections archive at http://gdo-dcp.ucllnl.org/downscaled_cmip3_projections/#Projections:%20Complete%20Archives.

years throughout the instrumental record have tended to build up and finally abate over an extended multiyear period. Historically, and especially during the early twenty-first century, Southwestern droughts have been exacerbated by unusually warm summer temperatures. This tendency could worsen in future decades: several twenty-first-century climate model simulations suggest that dry years will include anomalously warm summer temperatures even above and beyond the warming trend in the Southwest (Cayan et al. 2010). During extreme droughts, the deficit in soil moisture grows larger, and also grows in comparison to the deficit in precipitation. Although projected precipitation anomalies during dry spells do not change markedly from observed past conditions, other hydrologic measures—including soil moisture—become more depleted.

Human-induced climate change impacts on temperature, snowpack, and the timing of streamflow over the western United States have already been detected (Maurer, Stewart et al. 2007; Barnett et al. 2008; Bonfils et al. 2008; Pierce et al. 2008; Hidalgo et al. 2009),

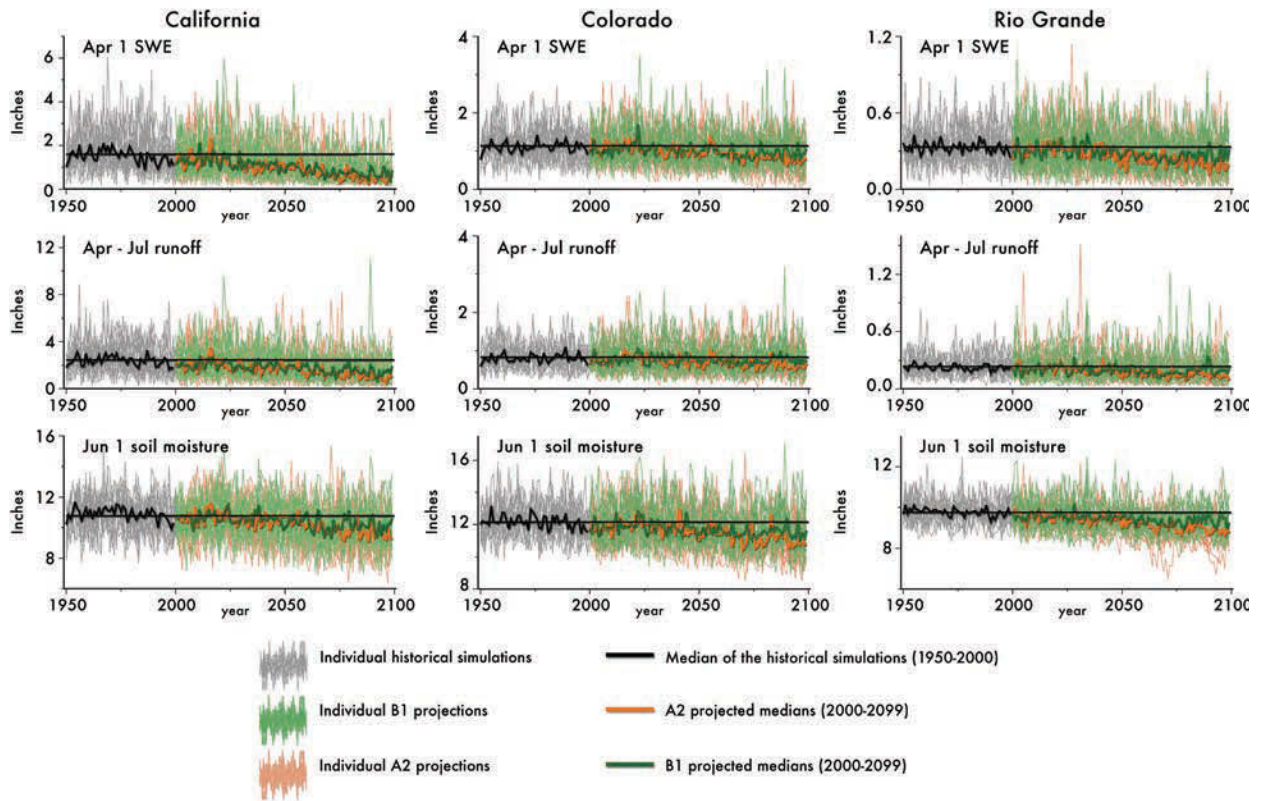
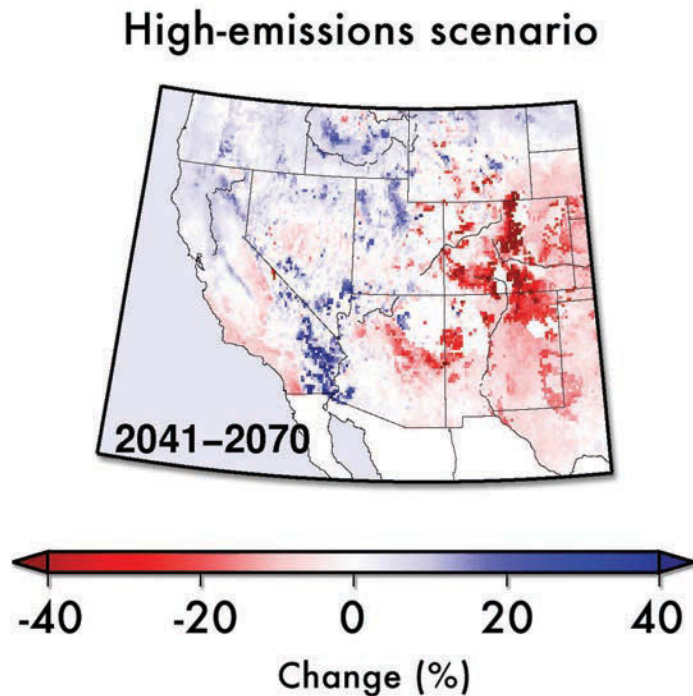


Figure 6.10 Spatially averaged values (in inches) for April 1 snow water equivalent (top), April–July runoff (middle) and June 1 soil moisture content (bottom). Averages are shown for California (left), Colorado (middle) and Rio Grande (right). Source: Bias Corrected and Downscaled World Climate Research Programme's CMIP3 Climate Projections archive at http://gdo-dcp.ucllnl.org/downscaled_cmip3_projections/#Projections:%20Complete%20Archives.

and as climate continues to warm there will be serious impacts on the hydrological cycle and water resources of the Southwest United States (Barnett et al. 2004; Seager et al. 2007). Water resource implications are described in Chapter 10. Downscaled temperature, precipitation, and modeled hydrologic measures already provide sufficient spatial detail to assess hydroclimatic effects that will be critical in planning for risks to water resources and ecosystems, risk of wildfire, and other key issues in the Southwest. A strong consensus among the model projections across the Southwest for substantially lower spring snowpack, lower spring-summer runoff, and drier summers underscores that traditional planning practices can no longer be supported (see Milly et al. 2008) or that the past can be assumed to be a reasonable representation of the future. Thus, past hydrological observations cannot sufficiently frame the risks of unfavorable future outcomes, such as an inability to meet demands for water.

Figure 6.11 High-emissions scenario mid-century (2041–2070) percent change from the historical period (1971–2000) for annual runoff. Data obtained from median of sixteen VIC simulations. Source: Bias Corrected and Downscaled World Climate Research Programme's CMIP3 Climate Projections archive at http://gdo-dcp.ucllnl.org/downscaled_cmip3_projections/#Projections:%20Complete%20Archives.



References

- Barnett, T., R. Malone, W. Pennell, D. Stammer, B. Semtner, and W. Washington. 2004. The effects of climate change on water resources in the west: Introduction and overview. *Climate Change* 62:1–11, doi:10.1023/B:CLIM.0000013695.21726.b8.
- Barnett, T. P., D. W. Pierce, H. Hidalgo, C. Bonfils, B. Santer, T. Das, G. Bala, et al. 2008. Human-induced changes in the hydrology of the western United States. *Science* 316:1080–1083.
- Barsugli, J. J., S-I. Shin, and P. D. Sardeshmukh. 2006. Sensitivity of global warming to the pattern of tropical ocean warming. *Climate Dynamics* 27:483–492, doi:10.1007/s00382-006-0143-7.
- Bieda, S.W. III, C. L. Castro, S. L. Mullen, A. Comrie, and E. Pytlak. 2009. The relationship of transient upper-level troughs to variability of the North American monsoon system. *Journal of Climate* 22:4213–4227.
- Bonfils, C., B. D. Santer, D. W. Pierce, H. G. Hidalgo, G. Bala, T. Das, T. P. Barnett, et al. 2008. Detection and attribution of temperature changes in the mountainous western United States. *Journal of Climate* 21:6404–6424, doi:10.1175/2008JCL12397.1.
- Castro, C. L., R. A. Pielke, Sr., and J. O. Adegoké. 2007. Investigation of the summer climate of the contiguous U.S. and Mexico using the Regional Atmospheric Modeling System (RAMS). Part I: Model climatology (1950–2002). *Journal of Climate* 20:3844–3865.
- Castro, C. L., R. A. Pielke, Sr., J. O. Adegoké, S. D. Schubert, and P. J. Pegion. 2007. Investigation of the summer climate of the contiguous U.S. and Mexico using the Regional Atmospheric Modeling System (RAMS). Part II: Model climate variability. *Journal of Climate* 20:3866–3887.
- Cayan, D. R., T. Das, D. W. Pierce, T. P. Barnett, M. Tyree and A. Gershunov. 2010. Future dryness in the southwest US and the hydrology of the early 21st century drought. *Proceedings of the National Academy of Sciences* 107:21271–21276.

- Cayan, D., M. Tyree, M. Dettinger, H. Hidalgo, T. Das, E. Maurer, P. Bromirski, N. Graham and R. Flick. 2009. *Climate change scenarios and sea level rise estimates for the California 2009 climate change scenarios assessment*. Final paper CEC-500-2009-014-F. Np: California Climate Change Center. <http://www.energy.ca.gov/2009publications/CEC-500-2009-014/CEC-500-2009-014-F.PDF>.
- Christensen, N., and D. P. Lettenmaier. 2007. A multimodel ensemble approach to assessment of climate change impacts on the hydrology and water resources of the Colorado River Basin. *Hydrology and Earth System Sciences* 11:1417–1434.
- Cook, E. R., C. Woodhouse, C. M. Eakin, D. M. Meko, and D. W. Stahle. 2004. Long-term aridity changes in the western United States. *Science* 306:1015–1018.
- Dai, A. 2006. Precipitation characteristics in eighteen coupled climate models. *Journal of Climate* 19:4605–4630.
- Das, T., H. Hidalgo, D. Cayan, M. Dettinger, D. Pierce, C. Bonfils, T.P. Barnett, G. Bala and A. Mirin. 2009. Structure and detectability of trends in hydrological measures over the western United States. *Journal of Hydrometeorology* 10:871–892, doi:10.1175/2009JHM1095.1.
- Das, T., D. W. Pierce, D. R. Cayan, J. A. Vano, and D. P. P. Lettenmaier. 2011. The importance of warm season warming to western U.S. streamflow changes. *Geophysical Research Letters* 38: L23403, doi:10.1029/2011GL049660.
- Dettinger, M. D., F. M. Ralph, T. Das, P. J. Neiman, and D. R. Cayan. 2011. Atmospheric rivers, floods and the water resources of California. *Water* 3:445–478.
- Dominguez, F., J. Cañon, and J. Valdes. 2009. IPCC-AR4 climate simulations for the southwestern U.S.: The importance of future ENSO projections. *Climatic Change* 99:499–514, doi:10.1007/s10584-009-9672-5.
- Dominguez, F., P. Kumar, and E. R. Vivoni. 2008. Precipitation recycling variability and ecoclimatological stability—A study using NARR data. Part II: North American monsoon region. *Journal of Climate* 21:5187–5203.
- Douglas, A. V., and P. J. Englehart. 2007. A climatological perspective of transient synoptic features during NAME 2004. *Journal of Climate* 20:1947–1954.
- Favre, A., and A. Gershunov. 2009. North Pacific cyclonic and anticyclonic transients in a global warming context: Possible consequences for western North American daily precipitation and temperature extremes. *Climate Dynamics* 32:969–987.
- Gangopadhyay, S., T. Pruiitt, L. Brekke, and D. Raff. 2011. Hydrologic projections for the western United States. *Eos Transactions AGU* 92:441, doi:10.1029/2011EO480001.
- Gao, X., J. Li, and S. Sorooshian. 2007. Modeling intraseasonal features of 2004 North American monsoon precipitation. *Journal of Climate* 20:1882–1896.
- Gutzler, D. S., H-K. Kim, R. W. Higgins, H-M. H. Juang, M. Kanamitsu, K. Mitchell, K. Mo, et al. 2005. The North American monsoon Model Assessment Project: Integrating numerical modeling into a field-based process study. *Bulletin of the American Meteorological Society* 86:1423–1429.
- Hawkins, E., and R. T. Sutton. 2009. The potential to narrow uncertainty in regional climate predictions. *Bulletin of the American Meteorological Society* 90:1095–1107.
- Hidalgo, H. G., T. Das, M. D. Dettinger, D. R. Cayan, D. W. Pierce, T. P. Barnett, G. Bala, et al. 2009. Detection and attribution of stream flow timing changes to climate change in the western United States. *Journal of Climate* 22:3838–3855, doi:10.1175/2009JCLI2470.1.
- Hoerling, M., and J. Eischeid. 2007. Past peak water in the Southwest. *Southwest Hydrology* 6 (1): 18–35.
- Hoerling, M., D. Lettenmaier, D. Cayan, and B. Udall. 2009. Reconciling projections of Colorado River streamflow. *Southwest Hydrology* 8 (3): 20–21, 31.

- Ikeda, K., R. Rasmussen, C. Liu, D. Gochis, D. Yates, F. Chen, M. Tewari, et al. 2010. Simulation of seasonal snowfall over Colorado. *Atmospheric Research* 97:462–477, doi:10.1016/j.atmosres.2010.04.010.
- Intergovernmental Panel on Climate Change (IPCC). 2007. *Climate change 2007: The physical science basis. Contribution of Working Group I to the Fourth Assessment Report of the Intergovernmental Panel on Climate Change*, ed. S. Solomon, D. Qin, M. Manning, Z. Chen, M. Marquis, K. B. Averyt, M. Tignor and H.L. Miller. Cambridge: Cambridge University Press. <http://www.ipcc.ch/ipccreports/ar4-wg1.htm>.
- Janowiak, J. E., V. J. Dagostaro, V. E. Kousky, and R. J. Joyce. 2007. An examination of precipitation in observations and model forecasts during NAME with emphasis on the diurnal cycle. *Journal of Climate* 20:1680–1692.
- Knowles, N., and D. R. Cayan. 2002. Potential effects of global warming on the Sacramento/San Joaquin watershed and the San Francisco estuary. *Geophysical Research Letters* 29:1891, doi:10.1029/2001GL014339.
- Knowles, N., M. D. Dettinger, and D. R. Cayan. 2006. Trends in snowfall versus rainfall in the western United States. *Journal of Climate* 19:4545–4559.
- Lambert, S. J. 1995. The effect of enhanced greenhouse warming on winter cyclone frequencies and strengths. *Journal of Climate* 8:1447–14452.
- Lambert, S. J., and J. C. Fyfe. 2006. Changes in winter cyclone frequencies and strengths simulated in enhanced greenhouse warming experiments: Results from the models participating in the IPCC diagnostic exercise. *Climate Dynamics* 26:713–728.
- Lang, T. J., D. A. Ahijevych, S. W. Nesbitt, R. E. Carbone, S. A. Rutledge, and R. Cifelli. 2007. Radar-observed characteristics of precipitating systems during NAME 2004. *Journal of Climate* 20:1713–1733.
- Laprise, R., R. de Elía, D. Caya, S. Biner, P. Lucas-Pincher, E. Diaconescu, M. Leduc, A. Alexandru, and L. Separovic. 2008. Challenging some tenets of regional climate modelling. *Meteorology and Atmospheric Physics* 100:3–22, doi:10.1007/s00703-0080292-9.
- Liang, X., D. P. Lettenmaier, E. Wood, and S. J. Burges. 1994. A simple hydrologically based model of land surface water and energy fluxes for General Circulation Models. *Journal of Geophysical Research* 99:14415–14428.
- Liang, X-L., J. Zhu, K. E. Kunkel, M. Ting, and J. X. L. Wang. 2008. Do CGCMs simulate the North American monsoon precipitation seasonal-interannual variability? *Journal of Climate* 21:4424–4448.
- Lu, J., G. A. Vecchi, and T. Reichler. 2007. Expansion of the Hadley cell under global warming. *Geophysical Research Letters* 34: L06805, doi:10.1029/2006GL028443.
- Maurer, E. P., L. Brekke, T. Pruitt, and P. B. Duffy. 2007. Fine-resolution climate projections enhance regional climate change impact studies. *EOS Transactions AGU* 88:504.
- Maurer, E. P., H. G. Hidalgo, T. Das, M. D. Dettinger, and D. R. Cayan. 2010. The utility of daily large-scale climate data in the assessment of climate change impacts on daily streamflow in California. *Hydrology and Earth System Sciences* 14:1125–1138.
- Maurer, E. P., I. T. Stewart, C. Bonfils, P. B. Duffy, and D. Cayan. 2007. Detection, attribution, and sensitivity of trends toward earlier streamflow in the Sierra Nevada. *Journal of Geophysical Research* 112: D11118, doi:10.1029/2006JD008088.
- Mearns, L. O., F. Giorgi, P. Whetton, D. Pabon, M. Hulme, and M. Lal, 2003. *Guidelines for use of climate scenarios developed from Regional Climate Model experiments*. N.p.: Data Distribution Centre of the Intergovernmental Panel on Climate Change. <http://www.ipcc-data.org/guidelines/RCM6.Guidelines.October03.pdf>.

- Mearns, L. O., W. Gutowski, R. Jones, R. Leung, S. McGinnis, A. Nunes, and Y. Qian. 2009. A regional climate change assessment program for North America. *Eos Transactions AGU* 90:311.
- Meehl, G. A., T. F. Stocker, W. D. Collins, P. Friedlingstein, A. T. Gaye, J. M. Gregory, A. Kitoh, et al. 2007. Global climate projections. In *Climate change 2007: The physical science basis. Contribution of Working Group I to the Fourth Assessment Report of the Intergovernmental Panel on Climate Change*, ed. S. Solomon, D. Qin, M. Manning, Z. Chen, M. Marquis, K.B. Averyt, M. Tignor and H.L. Miller, SM.10-1 – SM.10-8. Cambridge: Cambridge University Press. <http://www.ipcc.ch/pdf/assessment-report/ar4/wg1/ar4-wg1-chapter10-supp-material.pdf>.
- Milly, P. C. D., J. Betancourt, M. Falkenmark, R. M. Hirsch, Z. W. Kundzewicz, D. P. Lettenmaier, and R. J. Stouffer. 2008. Stationarity is dead: Whither water management? *Science* 319:573–574.
- Mote, P. W., A. F. Hamlet, M. P. Clark, and D. P. Lettenmaier. 2005. Declining mountain snowpack in western North America. *Bulletin of the American Meteorological Society* 86:39–49.
- Nakićenović, N., and R. Swart, eds. 2000. *Special report on emissions scenarios: A special report of Working Group III of the Intergovernmental Panel on Climate Change*. Cambridge: Cambridge University Press.
- Nesbitt, S. W., D. J. Gochis, and T. J. Lang. 2008. The diurnal cycle of clouds and precipitation along the Sierra Madre Occidental observed during NAME-2004: Implications for warm season precipitation estimation in complex terrain. *Journal of Hydrometeorology* 9:728–743.
- Pierce, D. W., T. P. Barnett, H. G. Hidalgo, T. Das, C. Bonfils, B. D. Santer, G. Bala, et al. 2008. Attribution of declining western U.S. snowpack to human effects. *Journal of Climate* 21:6425–6444, doi:10.1175/2008JCLI2405.1.
- Pierce, D. W., T. P. Barnett, B. D. Santer, and P. J. Gleckler. 2009. Selecting global climate models for regional climate change studies. *Proceedings of the National Academy of Sciences* 106:8441–8446, doi:10.1073/pnas.0900094106.
- Pierce, D. W., T. Das, D. R. Cayan, E. P. Maurer, N. L. Miller, Y. Bao, M. Kanamitsu, et al. 2012. Probabilistic estimates of future changes in California temperature and precipitation using statistical and dynamical downscaling. *Climate Dynamics* 39, published online, doi: 10.1007/s00382-012-1337-9.
- Ray, A. J., J. J. Barsugli, K. B. Averyt, K. Wolter, M. Hoerling, N. Doesken, B. Udall, and R. S. Webb. 2008. *Climate change in Colorado: A synthesis to support water resources management and adaptation*. Boulder, CO: Western Water Assessment. <http://cwcb.state.co.us/public-information/publications/Documents/ReportsStudies/ClimateChangeReportFull.pdf>.
- Ruff, T. W., Y. Kushnir, and R. Seager. 2012. Comparing 20th and 21st century patterns of inter-annual precipitation variability over the western United States and northern Mexico. *Journal of Hydrometeorology* 13:366–378.
- Salathé, E. P. Jr. 2006. Influences of a shift in North Pacific storm tracks on western North American precipitation under global warming. *Geophysical Research Letters* 33: L19820, doi:10.1029/2006GL026882.
- Santer, B. D., K. E. Taylor, P. J. Gleckler, C. Bonfils, T. P. Barnett, D. W. Pierce, T. M. L. Wigley, et al. 2009. Incorporating model quality information in climate change detection and attribution studies. *Proceedings of the National Academy of Sciences* 106:14778–14783, doi:10.1073/pnas.0901736106.
- Seager, R., M. Ting, I. Held, Y. Kushnir, J. Lu, G. Vecchi, H-P. Huang, et al. 2007. Model projections of an imminent transition to a more arid climate in southwestern North America. *Science* 316:1181–1184.

- Seager, R., and G. A. Vecchi. 2010. Greenhouse warming and the 21st century hydroclimate of southwestern North America. *Proceedings of the National Academy of Sciences* 107:21277–21282.
- U.S. Bureau of Reclamation (Reclamation). 2011a. *Literature synthesis on climate change implications for water and environmental resources*, 2nd ed. Technical Memorandum 86-68210-2010-03. Denver: Reclamation, Research and Development Office. <http://www.usbr.gov/research/docs/climatechangelitsynthesis.pdf>.
- . 2011b. *West-wide climate risk assessments: Bias-corrected and spatially downscaled surface water projections*. Technical Memorandum 86-68210-2011-01. Denver: Reclamation, Technical Service Center.
- Vano, J. A., T. Das, and D. P. Lettenmaier. 2012. Hydrologic sensitivities of Colorado River runoff to changes in precipitation and temperature. *Journal of Hydrometeorology* 13:932–949.
- Wi, S., F. Dominguez, M. Durcik, J. Valdes, H. Diaz, and C. L. Castro. 2012. Climate change projections of snowfall in the Colorado River Basin using dynamical downscaling. *Water Resources Research* 48: W05504.
- Wilby, R. L., S. P. Charles, E. Zorita, P. Whetton, and L. O. Mearns. 2004. *Guidelines for use of climate scenarios developed from statistical downscaling methods*. N.p.: IPCC Data Distribution Center. http://www.ipcc-data.org/guidelines/dgm_no2_v1_09_2004.pdf.
- Wood, A. W., L. R. Leung, V. Sridhar, and D. P. Lettenmaier. 2004. Hydrologic implications of dynamical and statistical approaches to downscaling climate model outputs. *Climatic Change* 62:189–216.
- Woodhouse, C.A., D. M. Meko, G. M. MacDonald, D. W. Stahle, and E. R. Cook. 2010. A 1,200-year perspective of 21st century drought in southwestern North America. *Proceedings of the National Academy of Sciences* 107:21283–21288.

Endnotes

- i The BCSD method removes bias in the climate model output by mapping from the probability distribution of a current climate simulation to the probability distribution of observations on a monthly basis.
- ii For downscaling simulated surface temperature from the GCMs, the BCSD methodology preserves GCM (large-scale) trends by removing them initially and adding them back after the downscaling is implemented. For downscaling simulated precipitation, no explicit step is included in BCSD to preserve the GCM trends, because trends are not so obviously present. Other inherent weaknesses of the BCSD approach are the assumption of climate “stationarity”—the idea that statistical relationships developed in a historical period are applicable to a future period—and the underestimation of variability (Wilby et al. 2004; Milly et al. 2008).
- iii VIC is a macroscale, distributed, physically based hydrologic model that balances both surface energy and water over a grid mesh. For this report, VIC simulations, run from BCSD downscaled precipitation and temperature data, were employed.
- iv CMIP3 is phase 3 of the World Climate Research Programme’s Coupled Model Intercomparison Project.
- v With a baseline of 65°F, heating degree days are the sum of the temperature differences of the daily mean temperature subtracted from 65°F, for all days when the mean temperature is less than 65°F. Cooling degree days are calculated similarly, but for when the mean temperature exceeds 65°F.

- vi Cyclones are the rapid circulation of winds around a low pressure center, traveling counterclockwise in the Northern Hemisphere and clockwise in the Southern Hemisphere. Anticyclones spiral out from a high pressure area and travel clockwise in the Northern Hemisphere and counterclockwise in the Southern Hemisphere.
- vii CNRM-C3 is the third version of a global ocean-atmosphere model originally developed at the Centre National de Recherches Meteorologiques, France.